processes

MDPI

Article

Microwave Drying of Sewage Sludge: Process Performance and Energy Consumption

Guangyu Wang, Kai Zhang *, Bocheng Huang, Kaihua Zhang and Cong Chao

Beijing Key Laboratory of Emission Surveillance and Control for Thermal Power Generation, North China Electric Power University, Beijing 102206, China; guangyu15@163.com (G.W.); 18186450097@163.com (B.H.); myzkh2@126.com (K.Z.); 50202852@ncepu.edu.cn (C.C.)

* Correspondence: kzhang@ncepu.edu.cn; Tel.: +010-61772413

Abstract: The microwave drying of sewage sludge is characterized by its speed and safety. A novel method for identifying free and bound water is proposed in this study. Experiments were performed to investigate the process performance and energy consumption in a microwave drying unit. The results indicate that the microwave drying process can be described in three stages, i.e., the preheating stage, constant-rate stage, and decreasing-rate stage. The preheating and constant-rate stages mainly remove free water, while the decreasing-rate stage mainly removes bound water. The Linear model effectively describes the kinetic processes in the constant-rate stage, and the modified Page I model is suitable for describing the decreasing-rate stage. The energy conversion process in microwave drying is explored, revealing that heat efficiency and energy consumption are consistent with microwave power changes. The heat efficiency in the constant-rate drying stage ranges from 60.33% to 71.01%, lower than that in the preheating stage but higher than that in the decreasing-rate stage. Energy consumption in the constant-rate stage ranges from 3.84 kJ/g to 8.20 kJ/g, significantly lower than in the other two stages. These results provide fundamental data for the industrial application of microwave drying of sludge and contribute to the advancement of microwave drying technology.

Keywords: sludge; microwave; drying; kinetics; energy consumption

Citation: Wang, G.; Zhang, K.; Huang, B.; Zhang, K.; Chao, C. Microwave Drying of Sewage Sludge: Process Performance and Energy Consumption. *Processes* **2024**, *12*, 432. https://doi.org/10.3390/pr12030432

Academic Editor: Vladimir S. Arutyunov

Received: 25 January 2024
Revised: 16 February 2024
Accepted: 18 February 2024
Published: 20 February 2024

1. Introduction

Sewage sludge is dramatically increasing worldwide due to urbanization and industrialization [1,2]. Drying serves as a preliminary procedure for utilizing sewage sludge, such as pyrolysis [3], gasification [4], and combustion [5]. The moisture within sludge has been categorized in various ways, such as Norinaga et al. [6] classifying it as free water, bound water, and non-frozen water. Allardice et al. [7] categorize it as free water, bound water, pore water, single-layer absorbed water, and multi-layer absorbed water, while Karthikeyan et al. [8] divide it into surface absorbed water, intergranular water, pore water, attached water, and internal absorbed water. In fact, free water and bound water are sufficient to describe the drying process of sludge [9,10]. Although many researchers [11–13] have attempted to determine different types of moisture content, the accuracy of test methods and results needs improvement [14].

Microwave drying offers a faster and more uniform alternative to traditional drying methods. Traditional drying methods require high temperatures of up to 200 °C or even 300 °C [15] and extended drying times [16–18], thereby reducing dryer efficiency. In contrast, microwave irradiation is gaining increasing attention due to its several advantages [19], including uniformity, selectivity, safety, rapidity, and instantaneity. Microwave heating, recognized as an efficient external field enhancement technology [20–23], employs electromagnetic waves ranging from 300 MHz to 300 GHz to transfer energy to polar molecules, such as water in wet materials. This process relies on the principle that energy conversion and transfer occur through intense friction and collision between molecules, resulting in the transmission of heat and moisture from the inside to the outside. The

"pumping effect" [24,25] of microwave heating increases the drying rate over a small temperature difference. Elenga et al. [26] and Bantle et al. [27] conducted a comparative analysis between microwave drying and conventional drying methods. Their finding largely favored the application of microwave drying for its ability to produce a high-quality final dried product. Similarly, Dominguez et al. [28] and Fang et al. [29] found a significant reduction in drying time compared to the hot air convective drying of sludge. Despite its advantages, the complexity of the microwave transmission process and its interaction with materials can result in uneven heating. More importantly, microwave drying technology is known for its high cost [30]. To improve the uniformity of temperature distribution and reduce energy consumption, scholars have proposed technologies such as continuous microwave drying [31], intermittent microwave drying [32], microwave vacuum drying [33], microwave-convection drying [34], and microwave-coupled fluidized bed drying [35]. However, these studies lack an in-depth analysis of the essence of heat and mass transfer in the three stages of the drying process.

Drying kinetics are crucial for gaining insights into the underlying drying mechanism. Based on research findings from conventional hot air drying, the microwave drying process of materials, such as lignite [36–38] or sludge [39,40], can be divided into three stages: preheating, constant-rate, and decreasing-rate stages. Some researchers [41–43] have further divided the decreasing-rate stage of lignite into two stages to account for the shrinkage effect observed during the drying process. Several drying models have been proposed and implemented, which can be classified into empirical [44] and mechanistic models [45,46]. In terms of empirical models, commonly known as drying kinetics, Lewis proposed the classic exponential model in 1921, which later became known as the Lewis model [47]. Subsequently, scholars have refined and improved models. Commonly used models include the Lewis model, Page model, modified Page I model, modified Page II model, and Linear model [47,48]. Some researchers [20,23,41,49] have integrated Fick's second law with the Arrhenius formula to further calculate the activation energy of moisture diffusion. In terms of mechanistic models, several models only implemented the heat transfer equation [50]. However, a combination of heat and mass transfer equations must be implemented [51] for microwave drying. The reaction engineering approach (REA) has been implemented in numerous challenging drying situations [52–55] and has achieved excellent simulation results. Current research on microwave drying kinetics primarily focuses on fitting experimental data with the aforementioned kinetic models and selecting the model that best matches the data. For example, Hatibaruah et al. [56] identified the Page model as suitable for tea, Kantrong et al. [57] suggested using the modified Page model (I) for shiitake mushrooms, while Arslan et al. [58] indicated that both the Page model and modified Page model (I) effectively describe onion slices.

Energy consumption significantly influences the efficiency of the microwave drying process. Hacifazlioglu et al. [59] found that the microwave drying of coal slime pellets at 700 W is faster than hot air drying at 150 °C. Meanwhile, Song et al. [23] observed a decrease in energy consumption of coal slime particles with a diameter of 50 mm as microwave power increased within the range of 320 to 800 W. In addition, they found that at 800 W, energy consumption increased with an increase in particle size within the range of 30 to 60 mm. Guo et al. [60] discovered that the energy consumption of microwave drying sludge decreased with an increase in microwave power and increased with an increase in mass within the range of 500 to 750 g. However, it decreased with an increase in mass within the range of 750 to 1250 g. High dehydration energy consumption poses a challenge to the widespread application of microwave drying technology. Accurate measurement of sludge energy consumption is the basis for improving microwave drying technology.

The aims of this study are to propose a method for testing moisture types in sludge, clarify the process performance of microwave drying sludge, study the microwave drying kinetics in the constant-rate stage and the decreasing-rate stage, and perform an analysis of energy consumption in microwave drying sludge.

2. Materials and Methods

2.1. Materials

The sample was received from a wastewater treatment plant located in Shanxi Province, China. The sample was stored in a sealed plastic drum, maintaining a cool, light-free environment. The initial moisture content was determined according to the ASTM D4442-07 standard [20]. Accordingly, the sample was dried in an oven set at 105 °C until a stabilized mass was achieved, which took approximately 24 h. The initial moisture content of the sludge was found to be 38.3 ± 0.3 wt.%. Table 1 presents the results of the proximate analysis of the samples.

Table 1. Proximate analysis of the sludge.

Sample	Proximate Analysis (wt.%, ad)			
	Moisture	Ash	Volatile Matter	Fixed Carbon
1	1.99	63.72	30.47	3.82
2	1.87	63.81	30.73	3.59
3	1.82	63.83	30.84	3.51
4	1.76	63.83	31.03	3.38
5	1.75	63.85	30.83	3.57
average	1.84 ± 0.09	63.81 ± 0.05	30.78 ± 0.20	3.57 ± 0.16

ad: air-dried basis.

2.2. Determining Moisture in the Sample Based on the Changes of Mass and Heat via TGA

To determine the free water and bound water in the sludge, a quantitative method is proposed using TGA (Thermogravimetric analysis) technology. The accuracy of the TGA method is measured using wet quartz sand and $CuSO_4 \cdot 5H_2O$. The theoretical weight loss can be calculated based on the $CuSO_4 \cdot 5H_2O$ dehydration process [61]. The results are shown in Figures A1 and A2. Wet quartz sand and copper sulfate pentahydrate are chosen because the water in wet quartz sand is 100% free water, while the water in copper sulfate pentahydrate is 100% bound water. Selecting these two substances simplifies the determination of the accuracy of the TGA method, as they represent extremes in moisture composition. They are ideal materials for validating the accuracy of the TGA method. The detailed process is as follows: The moisture types of the sludge samples were determined using a thermogravimetric analyzer (STA 449F3, NETZSCH, Selber, Germany). In this procedure, 20 ± 0.1 mg of the sample was put into a crucible, and the nitrogen flow rate was set to 20 mL/min. The device was purged with nitrogen for 5 to 10 min. The sample was dried at 25 to 35 °C for 4 to 5 h, followed by heating at a rate of 1 ± 0.1 °C /min from 25 to 35 °C to 100 to 110 °C, and further drying at 100 to 110 °C for 1 to 2 h. In addition, it is crucial to thoroughly mix the materials before the experiment and ensure that the thermal analysis instruments operate in a stable environment below 25 °C. During the experiment, minimizing movement is advised to reduce potential impacts. Experiments for each sample were measured at least three times, and the error was within ±3%.

The moisture within the sludge underwent evaporation under the predetermined temperature program. Due to the varying binding forces between solid particles and free water versus bound water, they can be distinguished according to TG (thermo-gravimetry) and DSC (differential scanning calorimetry) characteristics. Analyzing the thermal data of the sludge samples revealed that the first coincident peak point of DDTG (the second derivative of TG with respect to time) and DDSC (the first derivative of DSC with respect to time) corresponds to the dividing point between free water and bound water.

2.3. Experimental Equipment and Methods

Figure 1 illustrates the experimental setup for sludge microwave drying. The dimensions of the microwave equipment are 1100 × 1050 × 2000 mm. The setup comprises a microwave source, a microwave cavity, a dryer, an electronic balance, a fiber-optic thermometer, a power meter, an exhaust fan, and a computer. The microwave frequency is

2.45 GHz. The microwave power can be continuously adjusted within the range of 400 to 3000 W. Power consumption is recorded by the power meter. The dimensions of the microwave chamber are 600 × 650 × 675 mm. The microwave chamber is made of stainless steel to prevent any microwave leakage, and the dryer is made of quartz to hold the sludge samples. An electronic balance is used to measure the mass of the samples over time, with an error within ±0.01 g. Temperature is monitored through the use of three fiber-optic thermometers over time at different locations within the sample, with an error within ±0.1 °C. An exhaust fan maintains stable pressure in the microwave cavity. Microwave power, sample mass, and temperature are recorded by a computer in real time.

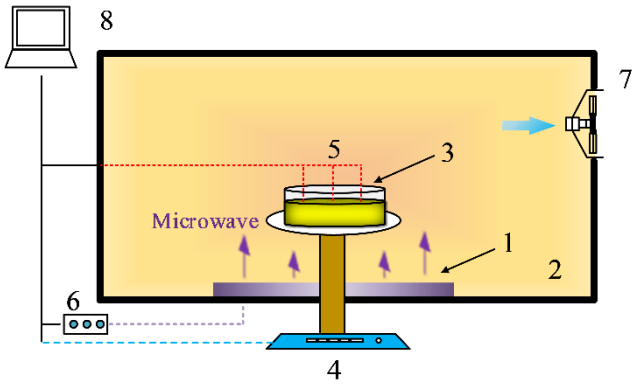

Figure 1. Schematic diagram of the microwave drying system; 1—microwave source; 2—microwave cavity; 3—dryer; 4—electronic balance; 5—fiber-optic thermometer; 6—power meter; 7—exhaust fan; 8—computer.

The sludge sample was evenly spread in the dryer before the start of each experiment. Three fiber-optic thermometers were then inserted into different locations of the sludge to monitor the temperature. The microwave oven chamber door was then closed slowly to minimize the impact on the electronic balance. The cooling water circulation device was turned on to cool the magnetron, the exhaust fan was turned on, and the instrument was preheated. The experiment was started after the instrument had operated normally for about 5 min to reach a stable state. Microwave power, mass, and temperature were measured using the power meter, electronic balance, and fiber-optic thermometers, respectively, with a sampling frequency of 10 times/min. The experiment concluded when no further reduction in the quality of the sludge was observed. After the test, any remaining materials were removed, and the microwave oven, fan, and circulating cooling water device were turned off. The process performance of the sludge in the microwave power range of 500 to 800 W was investigated in this study.

3. Results and Discussion

This study involves measuring the change in the mass and temperature of the sludge to investigate the characteristics of microwave drying, explore the microwave drying mechanisms, study the microwave drying kinetic model, and analyze the energy consumption of microwave drying sludge.

3.1. Changes of Temperature and Moisture Content in the Sludge Drying Process

Figure 2 shows the variation characteristics of temperature T and dry basis (db) moisture content of the 200 g sample. The dry basis moisture content is calculated as follows:

$$M_t = \frac{W_t - W_{d,s}}{W_{d,s}} \quad (1)$$

where M_t is the dry basis moisture content (g/g db), W_t is the mass of the sample at time t (g), $W_{d,s}$ is the mass of the dry sample (g), and t is the drying time (min).

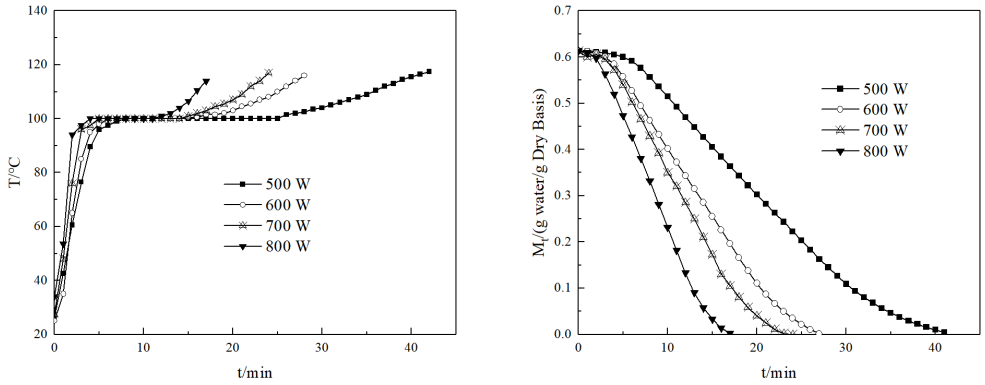

(**a**) (**b**)

Figure 2. Variation in moisture of sludge with temperature. (**a**) Temperature vs. drying time; (**b**) moisture content vs. drying time.

Figure 2a shows a sharp rise in sample temperature from 25 to 100 °C, followed by a subsequent increase after a certain point, depicting three distinct stages. Figure 2b indicates that the time required for complete drying of a 200 g sample decreased with increasing power. These results show that the drying rate of the sample increases with the increase in microwave power. Similar conclusions were drawn by Song et al. [23,30] on coal slime and lignite. Additionally, Mawioo et al. [40] and Bennamoun et al. [22] drew analogous conclusions in their investigations on sludge.

In the preheating stage, the sludge temperature sharply increases from room temperature to 100 °C, resulting in a rapid increase in drying rate. Initially, a small amount of water is removed, indicating that the absorbed microwave energy primarily contributes to sensible heat, elevating the sludge temperature. Due to the low partial pressure of water vapor in the surrounding environment, only a small amount of moisture in sludge is released from the sludge into the surrounding environment. The microwave energy absorbed by the sludge increases with increasing microwave power, leading to accelerated moisture evaporation and heating rates. This acceleration shortens the duration of the preheating stage. Once the sludge temperature reaches 100 °C, the microwave drying rate reaches its maximum, marking the transition to the constant-rate stage.

In the constant-rate stage, the sludge temperature is stable at 100 °C. This phase involves the rapid removal of free water between sludge particles, leading to a rapid reduction in M_t. The absorbed energy during this stage is entirely utilized as latent heat for evaporating moisture. Despite the ambient temperature being lower than 100 °C, the experiment reveals a few small water droplets on the surface. This suggests that the internal temperature is significantly higher than its surface temperature. The end of this stage is marked by the disappearance of water droplets on the surface of the sample, accompanied by a subsequent rise in temperature.

In the decreasing-rate stage, the temperature increases from 100 °C, and the drying rate decreases. This stage primarily removes surface-absorbed water and internal bound water from the sludge particles. Most moisture is removed during the constant-rate stage, mainly leaving behind bound water and the solid matrix. This suggests that the absorbed microwave energy is used both for evaporating moisture and increasing the sludge temperature.

3.2. Heat and Mass Transfer Process in Sludge

Microwave drying and hot air drying have significantly different heat and mass transfer mechanisms; however, sludge drying still exhibits three distinct stages in temperature and dry basis moisture content. This study takes into account the traditional drying stages:

preheating stages, constant-rate stage, and decreasing-rate stage. The drying rate and the moisture ratio are calculated as follows:

$$DR = \frac{M_t - M_{t+dt}}{dt} \tag{2}$$

$$MR = \frac{M_t - M_e}{M_0 - M_e} \tag{3}$$

where DR is the drying rate (g/(g db·min)), MR is the moisture ratio, M_t and M_{t+dt} are the dry basis moisture content of the sample at time t and time $t + dt$ (g/g db), M_0 is the initial dry basis moisture content of the sample (g/g db), and M_e is the dry basis moisture content at the end (g/g db). M_e can be regarded as 0 [20,62,63]. Therefore, MR can be simplified as follows:

$$MR = M_t / M_0 \tag{4}$$

The variation curve of dry basis moisture content in Figure 2b over time is differentiated to obtain the characteristic DR over time, as shown in Figure 3a. Subsequently, the corresponding relationship between water content (MR) and drying rate (DR) is obtained (Figure 3b). Figure 4 shows the determination results of free water and bound water content in sludge during the microwave drying process. The following provides a detailed analysis of microwave drying sludge.

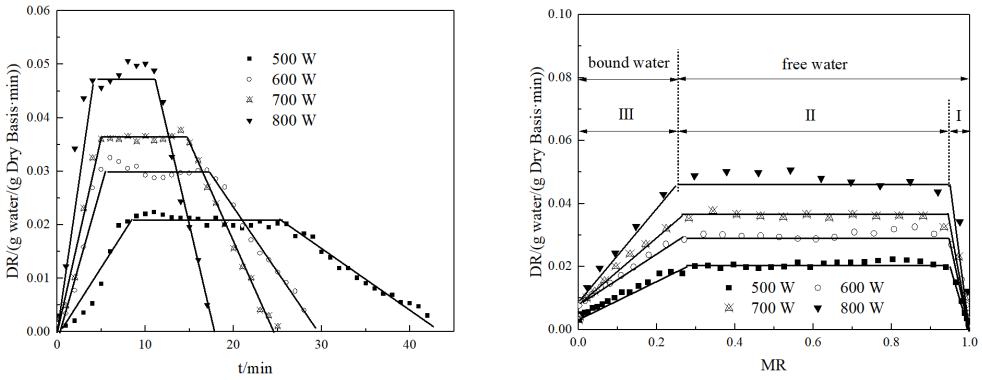

Figure 3. Microwave drying curves for sludge. (**a**) Drying rate vs. drying time; (**b**) drying rate vs. moisture ratio.

In the preheating stage, as shown in Figure 3a, the durations of this stage at 500 W, 600 W, 700 W, and 800 W are 8.1 min, 6.4 min, 5.0 min, and 4.1 min, respectively. In Figure 4a, the total moisture content of the sample is 37.50 wt.%, with the free water content of the sludge sample at 29.01 wt.%, and the bound water content is 8.49 wt.%. In Figure 4b, the total moisture content of the sample is 32.12 wt.%, with the free water content of the sludge sample at 23.90 wt.%, and the bound water content at 8.22 wt.%. Comparing Figure 4a,b, the bound water content remains unchanged, while the free water content decreases, indicating the removal of a small amount of free water during this stage. The microwave energy absorbed by the sludge increases with the increase in microwave power, which leads to the acceleration of the moisture evaporation rate and heating rate. It will shorten the duration of the preheating stage. Once the microwave drying rate reaches its maximum, this stage ends.

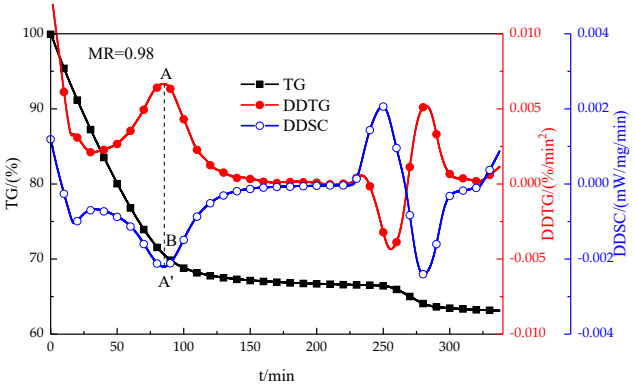

(**a**)

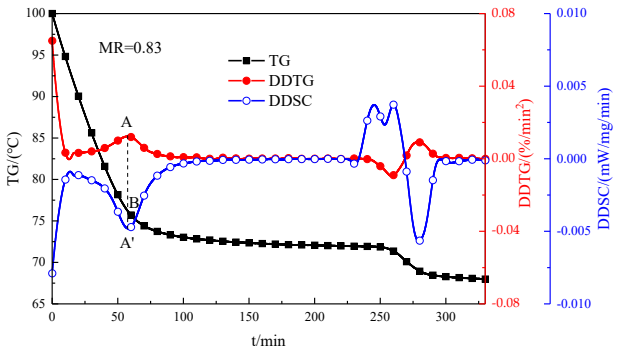

(**b**)

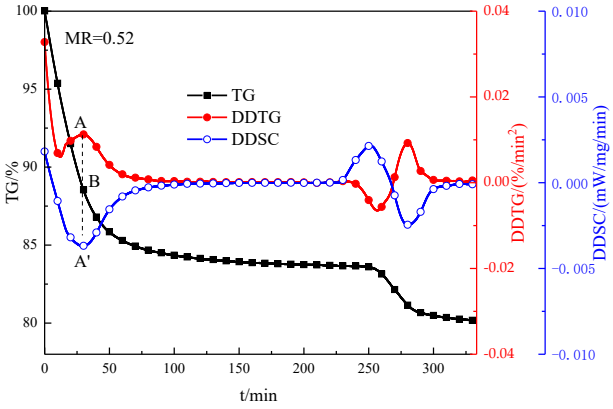

(**c**)

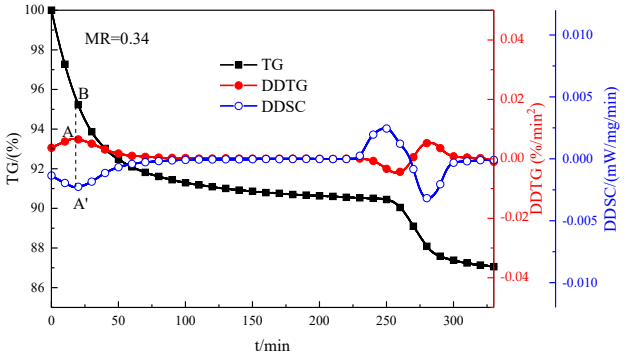

(**d**)

Figure 4. *Cont.*

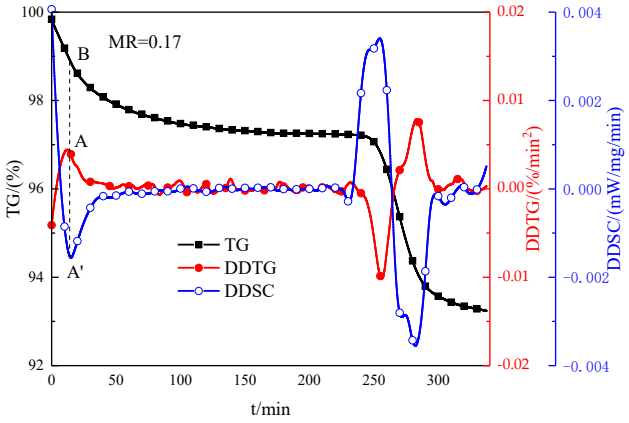

(**e**)

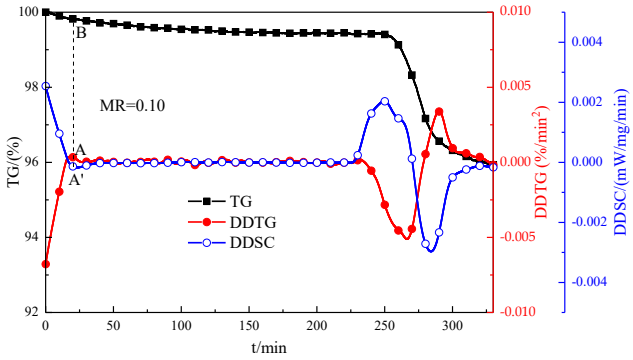

(**f**)

Figure 4. Results of moisture content determination of the sludge sample. (**a**) Determination of sludge moisture content (MR = 0.98); (**b**) determination of sludge moisture content (MR = 0.83); (**c**) determination of sludge moisture cosntent (MR = 0.52); (**d**) determination of sludge moisture content (MR = 0.34); (**e**) determination of sludge moisture content (MR = 0.17); (**f**) determination of sludge moisture content (MR = 0.10).

In the constant-rate stage, as shown in Figure 3a,b, the durations of this stage at 500 W, 600 W, 700 W, and 800 W are 18.5 min, 12.2 min, 11.1 min, and 8.5 min, respectively. The corresponding drying rates are 0.021 g/(g db·min), 0.029 g/(g db·min), 0.038 g/(g db·min), and 0.047 g g/(g db·min). In Figure 4c, the total moisture content of the sample is 20.02 wt.%, the free water content is 11.15 wt.%, and the bound water content is 8.87 wt.%. In Figure 4d, the total moisture content of the sample is 13.04 wt.%, the free water content is 4.61 wt.%, and the bound water content is 8.43 wt.%. By comparing Figure 4b–d, the bound water content remains unchanged, while the free water content drops significantly in the constant-rate stage, indicating that the moisture removed in this stage is mainly free water. The results show that the microwave energy absorbed by the sample in the constant-rate stage is entirely used for evaporating moisture in the form of latent heat. As the sample absorbs more microwave energy, its drying rate increases with increasing microwave power, resulting in a shorter duration of this stage. After a certain period of stability, this stage ends, and the process enters the decreasing-rate stage, where its drying rate begins to decrease.

In the decreasing-rate stage, as shown in Figure 3a, the durations of this stage at 500 W, 600 W, 700 W, and 800 W are 15.7 min, 11.2 min, 8.9 min, and 5.0 min, respectively. In Figure 4e, the total moisture content of the sample is 6.71 wt.%, the free water content is 1.00 wt.%, and the bound water content is 5.71 wt.%. In Figure 4f, the total moisture content of the sample is 4.10 wt.%, the free water content is 0.21 wt.%, and the bound water

content is 3.89 wt.%. Comparing Figure 4e,f, the rapid decrease in bound water content indicates that this stage removes the bound water. The main reasons for the decrease in drying rate are as follows: (1) The bound water in the sludge is attached to the interior or the surface of the solid matrix via chemical or hydrogen bonds [10], requiring more energy to break than free water. (2) The dielectric constant of the matrix is much smaller than that of water [42,64]. Therefore, the overall dielectric constant of the sludge gradually decreases with decreasing moisture content, leading to a decrease in the absorbed microwave energy and water evaporation as the drying progresses. (3) The diffusion mechanism of moisture in the pores of the solid matrix changes from molecular diffusion to a combination of molecular diffusion and Knudsen diffusion [65], causing the drying rate to decrease.

3.3. Microwave Drying Kinetics in Sludge

The aforementioned results indicate that sludge dehydration mainly occurs in the constant-rate and decreasing-rate stages; however, the drying mechanism differs significantly between these two stages.

3.3.1. Constant-Rate Stage

Five drying models are used to fit all drying experiments to determine the drying kinetics in the constant-rate stage, as shown in Table 2. The suitability of each model was evaluated according to the coefficient of determination (R^2), the reduced chi-square (χ^2), and the residual sum of squares (*RSS*). Higher values of R^2 and lower values of χ^2 and *RSS* indicated better goodness of fit.

Table 2. Statistical fitting results of the mathematical models in the constant-rate stage.

Model	Model Equation	P/W	R^2	χ^2	*RSS*	Coefficients
Lewis	$MR = exp(-kt)$	500	0.798	0.008	0.153	$k = 0.033$
		600	0.820	0.007	0.097	$k = 0.050$
		700	0.811	0.007	0.080	$k = 0.057$
		800	0.796	0.007	0.053	$k = 0.078$
Page	$MR = exp(-kt^n)$	500	0.998	4.833×10^{-5}	8.699×10^{-4}	$k = 0.002$, $n = 1.905$
		600	0.998	6.537×10^{-5}	7.845×10^{-4}	$k = 0.004$, $n = 1.914$
		700	0.998	4.656×10^{-5}	4.510×10^{-4}	$k = 0.005$, $n = 2.008$
		800	0.998	6.096×10^{-5}	3.657×10^{-4}	$k = 0.006$, $n = 2.155$
Modified Page I	$MR = exp(-(kt)^n)$	500	0.998	4.533×10^{-5}	8.099×10^{-4}	$k = 0.042$, $n = 1.905$
		600	0.998	6.537×10^{-5}	7.145×10^{-4}	$k = 0.062$, $n = 1.914$
		700	0.998	4.178×10^{-5}	4.225×10^{-4}	$k = 0.073$, $n = 2.008$
		800	0.998	6.596×10^{-5}	3.988×10^{-4}	$k = 0.098$, $n = 2.155$
Modified Page II	$MR = aexp(-kt^n)$	500	0.999	3.479×10^{-5}	5.914×10^{-4}	$a = 1.034$, $k = 0.002$, $n = 1.848$
		600	0.998	6.589×10^{-5}	7.248×10^{-4}	$a = 1.017$, $k = 0.004$, $n = 1.871$
		700	0.998	5.988×10^{-5}	4.784×10^{-4}	$a = 0.997$, $k = 0.005$, $n = 2.018$
		800	0.998	3.997×10^{-5}	1.998×10^{-4}	$a = 0.958$, $k = 0.006$, $n = 2.154$
Linear	$MR = at + b$	500	0.999	1.658×10^{-5}	2.984×10^{-4}	$a = -0.033$, $b = 1.172$
		600	0.999	1.031×10^{-5}	1.238×10^{-4}	$a = -0.048$, $b = 1.148$
		700	0.999	1.156×10^{-6}	1.545×10^{-5}	$a = -0.059$, $b = 1.133$
		800	0.999	1.559×10^{-5}	9.356×10^{-5}	$a = -0.078$, $b = 1.167$

Note: t and k refer to the drying time (min) and drying rate constant (min^{-1}), respectively. a, b, and n are fitting coefficients.

The linear model exhibits better performance in this stage. The values of R^2, χ^2 and *RSS* for the linear model were in the range of 0.999 to 0.999, 1.156×10^{-6} to 1.658×10^{-5}, and 1.545×10^{-5} to 2.984×10^{-4}, respectively. With higher R^2 and lower χ^2 and *RSS* than other models, the linear model is the best fit. The linear relationship between *MR* and time indicated a constant drying rate in the constant-rate stage, consistent with the variation law of the drying rate during this stage shown in Figure 3a. This reason was attributed to the constant temperature during this stage, where all the microwave energy was used for free water evaporation. Furthermore, the equations for linear models for the constant-rate

drying stages at 500 W, 600 W, 700 W, and 800 W were $MR = -0.033t + 1.172$, $MR = -0.048t + 1.148$, $MR = -0.059t + 1.133$ and $MR = -0.0787t + 1.167$, respectively. A comparison between the experimental MR and MR predicted by the linear model in the constant-rate stage is shown in Figure 5.

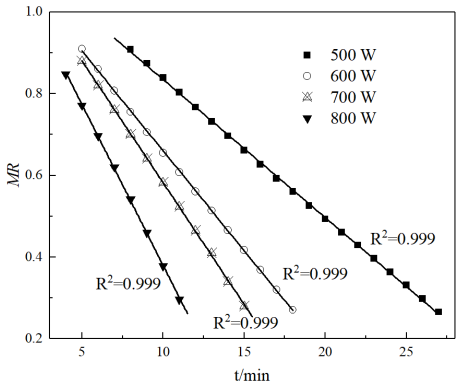

Figure 5. Comparison between the experimental moisture ratios and the moisture ratios predicted by the linear model in the constant-rate stage.

3.3.2. *Decreasing-Rate Stage*

The five models shown in Table 2 were used to analyze the decreasing-rate stage. The results are shown in Table 3, indicating that the Modified Page I model performed best in terms of describing the decreasing-rate stage. The values of R^2, χ^2 and *RSS* for the Modified Page I model ranged from 0.993 to 0.997, 1.417×10^{-5} to 4.386×10^{-5} and 5.669×10^{-5} to 3.618×10^{-4}, respectively. The drying rate constants for power levels of 500 W, 600 W, 700 W, and 800 W in the decreasing-rate stage were 0.040, 0.053, 0.066, and 0.081 min^{-1}, respectively. Furthermore, the equations for the Modified Page I models for the decreasing-rate drying stages at 500 W, 600 W, 700 W, and 800 W were $MR = \exp(-(0.040t)^{2.759})$, $MR = \exp(-(0.053t)^{3.254})$, $MR = \exp(-(0.066t)^{3.316})$, and $MR = \exp(-(0.081t)^{3.442})$, respectively. A comparison between the experimental MR and MR predicted by the Modified Page I model in the decreasing-rate stage is shown in Figure 6.

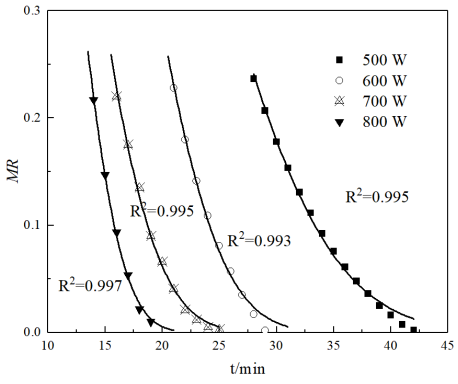

Figure 6. Comparison between the experimental moisture ratios and moisture ratios predicted by the Modified Page I model in the decreasing-rate stage.

Table 3. Statistical fitting results of the mathematical models in the decreasing-rate stage.

Model	Model Equation	P/W	R^2	χ^2	*RSS*	Coefficients
Lewis	$MR = exp(-kt)$	500	0.620	0.002	0.029	k = 0.067
		600	0.550	0.002	0.024	k = 0.094
		700	0.712	0.001	0.016	k = 0.121
		800	0.529	0.002	0.015	k = 0.143
Page	$MR = exp(-kt^n)$	500	0.995	2.852×10^{-5}	3.708×10^{-4}	$k = 6.875 \times 10^{-5}$, n = 1.789
		600	0.992	5.366×10^{-5}	4.293×10^{-4}	$k = 7.059 \times 10^{-5}$, n = 3.155
		700	0.991	4.956×10^{-5}	4.255×10^{-4}	$k = 1.217 \times 10^{-4}$, n = 3.324
		800	0.998	1.449×10^{-5}	5.798×10^{-5}	$k = 1.749 \times 10^{-4}$, n = 3.414
Modified Page I	$MR = exp(-(kt)^n)$	500	0.995	2.784×10^{-5}	3.618×10^{-4}	k = 0.040, n = 2.759
		600	0.993	4.386×10^{-5}	3.070×10^{-4}	k = 0.053, n = 3.254
		700	0.995	3.018×10^{-5}	2.652×10^{-4}	k = 0.066, n = 3.316
		800	0.997	1.417×10^{-5}	5.669×10^{-5}	k = 0.081, n = 3.442
Modified Page II	$MR = aexp(-kt^n)$	500	0.992	4.880×10^{-5}	5.856×10^{-4}	a = 2.636, k = 0.001, n = 2.210
		600	0.986	1.044×10^{-4}	7.307×10^{-4}	a = 2.494, k = 0.002, n = 2.241
		700	0.992	5.485×10^{-5}	1.985×10^{-4}	a = 2.021, k = 0.003, n = 2.805
		800	0.996	3.664×10^{-5}	1.099×10^{-4}	a = 1.582, k = 0.004, n = 2.809
Linear	$MR = at + b$	500	0.955	2.483×10^{-4}	0.003	a = -0.016, b = 0.667
		600	0.953	3.136×10^{-4}	0.002	a = −0.024, b = 0.721
		700	0.930	4.956×10^{-4}	0.003	a = −0.027, b = 0.642
		800	0.946	4.252×10^{-4}	0.002	a = −0.041, b = 0.774

Note: t and k refer to the drying time (min) and drying rate constant (min^{-1}), respectively. a, b, and n are fitting coefficients.

The apparent activation energy can be calculated based on the drying rate constant of the Modified Page I model. The following modified Arrhenius formula proposed by Ozbek et al. [66] was used:

$$k = k_0 \exp\left(\frac{-E_a W_0}{P}\right) \quad (5)$$

where k is the drying rate constant (min^{-1}), k_0 is the pre-exponential factor (min^{-1}), E_a is the apparent activation energy (W/g), P is the microwave power (W), and W_0 is the initial mass of the sample (g).

As shown in Figure 7, the correlation coefficient R^2 was 0.99. The apparent activation energy of sludge in the decreasing-rate stage was 4.68 W/g according to Equation (5).

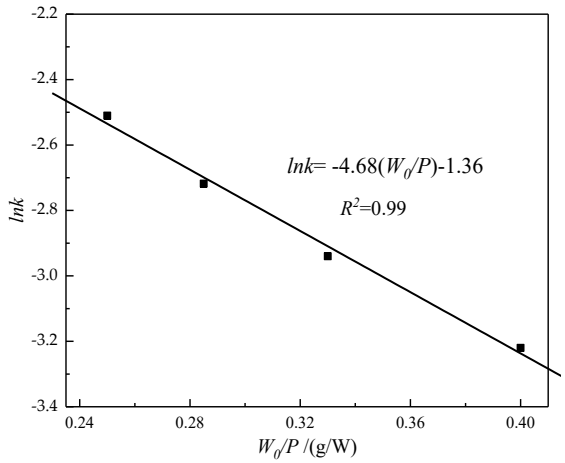

Figure 7. Fitting *lnk* vs. W_0/p in the decreasing-rate stage.

3.4. Analysis of Energy Consumption

During the sludge drying process, only a portion of the microwave energy is absorbed by the wet materials, while the remaining energy is dissipated into the surrounding environment and supporting components. In addition, electrical losses in the equipment

and microwave leakage from the device also lead to inevitable energy consumption. To improve the economic efficiency of the drying process, appropriate measures should be taken to reduce energy consumption.

3.4.1. Energy Transfer Process Analysis

As shown in Figure 8, the energy conversion process in the microwave drying of sludge mainly includes three steps: (1) Electric energy is converted into microwaves in the microwave cavity. (2) Sludge absorbs microwaves and converts them into heat. (3) The heat energy converted by the sample heats the sample, causing water to evaporate. In step 1, the electric power input of the microwave drying device is P_0. The real output power of the microwaves in the microwave cavity is P_{real}. Energy loss in this step is mainly due to equipment consumption P_3, including heat loss from the magnetron during operation and power loss from motors, fans, and bulbs within the device. In step 2, the heat absorbed and converted by the sample is P_h, while the energy loss mainly occurs due to microwave loss P_4. In step 3, the heat utilized for water evaporation is latent heat P_1 and sensible heat P_2, and the heat lost to the surrounding environment is P_5.

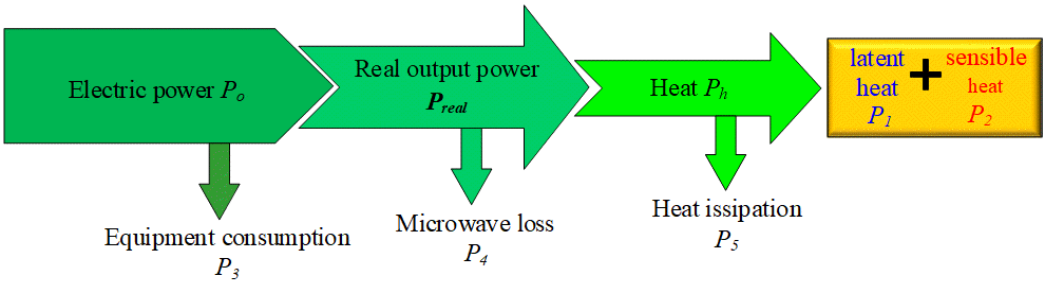

Figure 8. Schematic diagram of the energy conversion process.

The efficiencies of the device and heat utilization were calculated via the following equations:

$$\eta_{device} = P_{real} / P_0 \quad (6)$$

$$\eta = (P_1 + P_2) / P_{real} \quad (7)$$

where η_{device} is the efficiency of the drying device (%), η is the efficiency of heat (%), and P_0 is the electrical power consumed by the device, measured by the power meter in Figure 1; the detailed measurement results are shown in Table A1. P_{real} is the real output power of microwave (W), P_1 is the latent heat required for water evaporation (W), and P_2 is the sensible heat required for the rise in sludge temperature (W). The real output power P_{real} is measured according to GB/T18800-2017 [36]; detailed measurement steps and results can be found in Table A2.

Energy consumption is defined as the electric energy consumed by the evaporation of moisture per unit mass:

$$q = E / \Delta m \quad (8)$$

where q is the energy consumption (kJ/g [H_2O]), Δm is the mass of moisture removed from the sludge (g), and E is the total electrical energy consumed by the microwave equipment (kJ).

Table 4 presents the real microwave output power under different power settings. The results indicate that η_{device} increases with an increase in the microwave power. This is because the efficiency of converting electrical energy into microwaves gradually increases with increasing microwave power [60].

Table 4. Real output microwave power and efficiency of the device.

P (W)	P_0 (W)	P_{real} (W)	η_{device} (%)
500	329	138	41.9
600	364	200	54.9
700	399	248	62.1
800	437	359	82.3

Note: P is the setting microwave power (W).

The microwaves absorbed by the sludge can result in water evaporation and an increase in temperature. The total heat absorbed by the sludge is expressed as follows:

$$P_{s,t} = P_1 + P_2 = \left[(m_t - m_{t+dt}) \times \Delta H_v + \left(\frac{m_t + m_{t+dt}}{2} \times C_{s,t} \times (T_{t+dt} - T_t) \right) \right] / dt \quad (9)$$

where $P_{s,t}$ is the total heat absorbed by the sludge at time t (W), $C_{s,t}$ is the specific heat of sludge at time t (J/(kg·K)), T_t and T_{t+dt} are the temperatures of the sample at time t and $t + dt$ (°C), respectively, and ΔH_v is the latent heat of water (J/kg), which is 2.257×10^6 J/kg.

$C_{s,t}$ and $C_{ds,t}$ can be expressed as follows:

$$C_{s,t} = \frac{M_t}{1 + M_t} C_{water} + \frac{1}{1 + M_t} C_{ds,t} \quad (10)$$

$$C_{ds,t} = 3.2T_t + 1077 \quad (11)$$

where $C_{s,t}$ is the specific heat of sludge sample at time t (J/(kg·K)), C_{water} is the specific heat of water (J/(kg·K)), which is taken as 4200 J/(kg·K), and $C_{ds,t}$ is the specific heat of the dry sludge at time t (J/(kg·K)).

3.4.2. Efficiency of Heat and Energy Consumption

Figure 9 illustrates the variations in heat efficiency and energy consumption, respectively. The results indicate that the heat efficiency decreases during both the preheating and decreasing-rate stages but remains stable during the constant-rate stage. However, the energy consumption remains stable at a low value during the constant-rate stage, while it is relatively high during the preheating stage and decreasing-rate stage.

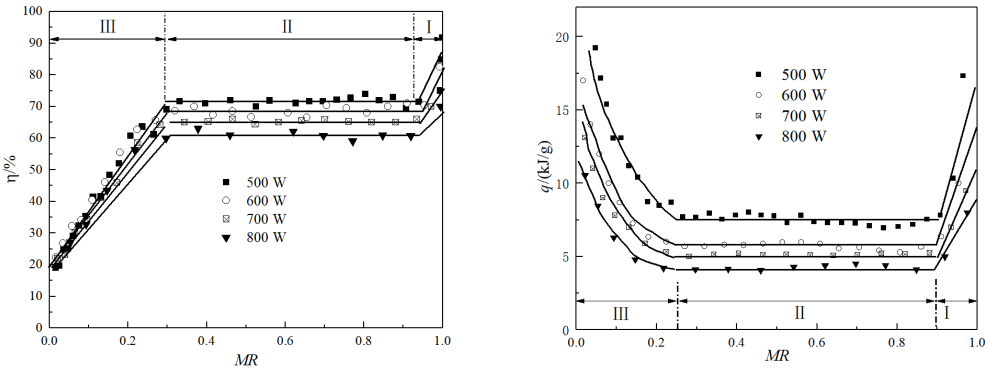

Figure 9. Heat efficiency and energy consumption vs. *MR*. (**a**) Heat efficiency vs. *MR*; (**b**) energy consumption vs. *MR*.

In the preheating stage, microwave energy is used to increase the sensible heat needed for temperature rise, with only a small portion allocated to the latent heat required for water evaporation. Due to the initially low temperature of the sludge, minimal heat is lost to the environment and the bottom support. However, heat loss increases as the drying process advances. This is attributed to the drying temperature, resulting in a gradual

decrease in heat efficiency. As a smaller amount of microwave energy is used for water evaporation, the energy consumption is relatively high. Nonetheless, DR increases as the drying progresses, causing q to decrease.

In the constant-rate stage, Figure 9a shows that the heat efficiency at 500 W, 600 W, 700 W, and 800 W is 71.01%, 68.34%, 65.40%, and 60.33%, respectively. Figure 9b shows that the energy consumption at 500 W, 600 W, 700 W, and 800 W is 8.20 kJ/g, 6.78 kJ/g, 4.92 kJ/g, and 3.84 kJ/g, respectively. In this stage, all energy is used as the latent heat required for water evaporation. Figure 2a indicates that the temperature remains stable at 100 °C, and Figure 3a shows that the drying rate of the sludge also remains stable during this stage. By combining Equations (7) and (9), the theoretical value of heat efficiency can be seen to be constant. Energy consumption is the lowest during this stage because all the consumed energy is used as the latent heat required for free water evaporation, maintaining a high drying level and significantly reducing energy consumption in this stage.

In the decreasing-rate stage, as the temperature of the sludge increases, more and more heat is lost to the environment and the bottom bracket. As a result, the heat efficiency gradually decreases as the drying progresses. The main reasons for the increase in energy consumption are as follows: The dielectric constant of the solid matrix is much smaller than that of water [42,64]; therefore, the microwave energy decreases with a decrease in M_t; moisture is mainly present in the form of bound water, which requires more energy to evaporate than free water; microwave energy is used to evaporate the moisture as well as increase the temperature; the drying rate of the sludge gradually decreases as the drying progresses.

The heat efficiency gradually decreases with an increase in microwave power. This is attributed to the increase in microwave leakage in the device with increasing microwave power. Additionally, energy consumption decreases as microwave power increases. Other scholars [23,60,67] have also reached similar conclusions. The reason may be that the heat efficiency decreases with an increase in the microwave power but the efficiency of the device increases with an increase in microwave power, as shown in Table 4. This leads to a decrease in energy consumption. At the same time, the "pumping effect" [24,25] is enhanced with an increase in microwave power, accelerating the drying process and reducing energy consumption.

4. Conclusions

The characteristics of sludge microwave drying, including process performance, kinetics, and energy consumption during different stages, were thoroughly analyzed in this study. The main conclusions are as follows:

(1) A precise method for identifying the types of moisture in sludge is proposed, allowing accurate measurement of changes in free water and bound water content during the microwave drying process. Free water is primarily removed during the preheating and constant-rate stages, while bound water is primarily removed during the decreasing-rate stage.

(2) The microwave drying of sludge can be described in three stages: preheating, constant-rate, and decreasing-rate drying stages. During the preheating stage, the temperature rises sharply to 100 °C, and the drying rate accelerates rapidly. The constant-rate stage maintains a stable temperature and consistent drying rate. The decreasing-rate stage sees a temperature rise again, and the drying rate gradually decreases.

(3) Various models, including the Lewis model, Page model, modified Page I model, and modified Page II model, are applied to fit the drying data. Although some models show reasonable agreement, the linear model proves to be the best fit in the constant-rate stage, and the modified Page I model is optimal for the decreasing-rate stage. The apparent activation energy of moisture evaporation in the decreasing-rate stage is 4.68 W/g.

(4) Heat efficiency and energy consumption are consistent with microwave power changes. Heat efficiency in the constant-rate drying stage ranges from 60.33% to 71.01%, which

is lower than that in the preheating stage but higher than that in the decreasing-rate stage. Energy consumption in the constant-rate drying stage ranges from 3.84 kJ/g to 8.20 kJ/g, which is significantly lower than in the other two stages.

Author Contributions: Conceptualization, K.Z. (Kai Zhang), K.Z. (Kaihua Zhang) and C.C.; Data curation, B.H.; Formal analysis, G.W.; Funding acquisition, K.Z. (Kai Zhang); Investigation, G.W.; Methodology, G.W. and B.H.; Project administration, K.Z. (Kai Zhang); Resources, K.Z. (Kai Zhang) and K.Z. (Kaihua Zhang); Software, B.H.; Supervision, K.Z. (Kai Zhang) and K.Z. (Kaihua Zhang); Validation, B.H.; Visualization, G.W. and B.H.; Writing—original draft, G.W. and C.C.; Writing—review and editing, G.W. All authors have read and agreed to the published version of the manuscript.

Funding: This research was funded by the National Natural Science Foundation of China, grant number U1910215.

Data Availability Statement: Data are unavailable due to privacy and ethical restrictions.

Conflicts of Interest: The authors declare no conflicts of interest.

Appendix A

Figure A1 shows the results of thermogravimetric analysis on the wet quartz sand sample. As shown in Figure A1a, the total moisture content is 19.50 wt.%. In Figure A1b, point A is the first peak point of DDTG, with a corresponding time of 78.3 min, and point A′ signifies the first peak point of DDSC, with a corresponding time of 79.2 min. The times corresponding to A and A′ are very close, and their average value is 78.7 min, which corresponds to point B. Point B is defined as the dividing point between free water and bound water. The free water content of the wet quartz sand sample is observed to be 19.15 wt.%. Theoretically, the free water content of the wet quartz sand is expected to be 19.50 wt.%, resulting in a relative error of 1.79%.

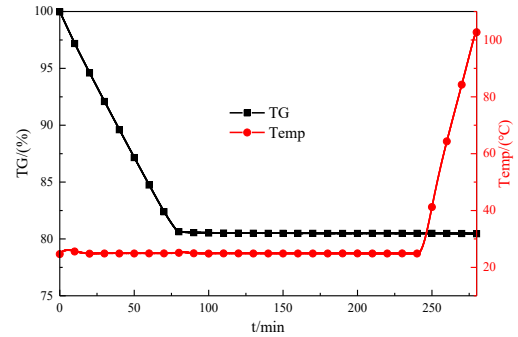

(**a**)

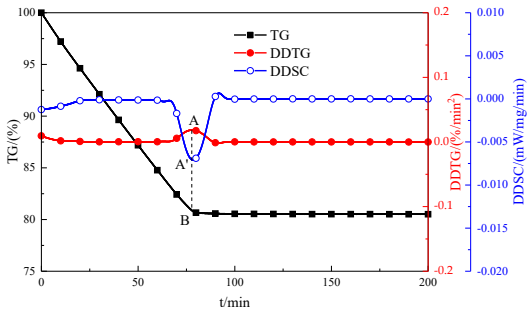

(**b**)

Figure A1. Thermal analysis results of the wet quartz sand sample. (**a**) Raw data for thermal analysis of the wet quartz sand sample; (**b**) thermal analysis data processing of the wet quartz sand sample.

Figure A2 shows the results of thermogravimetric analysis on the $CuSO_4 \cdot 5H_2O$ sample. In Figure A2a, the total moisture content of the sample is 28.61 wt.%. As shown in Figure A2b, point A is the first peak point of DDTG, with a corresponding time of 24.4 min, and point A′ is the first peak point of DDSC, with a corresponding time of 25.1 min. The times corresponding to A and A′ are very close, and their average value is 24.7 min, which corresponds to point B. It can be observed that the bound water content is 28.35 wt.%.

The drying process of $CuSO_4 \cdot 5H_2O$ is as follows:

$$CuSO_4 \cdot 5H_2O \rightarrow CuSO_4 \cdot 3H_2O + 2H_2O(g) \quad \text{(A1)}$$

$$CuSO_4 \cdot 3H_2O \rightarrow CuSO_4 \cdot H_2O + 2H_2O(g) \quad \text{(A2)}$$

$$CuSO_4 \cdot H_2O \rightarrow CuSO_4 + H_2O(g) \quad \text{(A3)}$$

$CuSO_4 \cdot 5H_2O$ loses four water molecules when dried at 100 °C; the reaction temperature in reaction (Al) is 35 °C, and the theoretical weight loss is 14.40 wt.%. The reaction temperature in reaction (A2) is in the range of 35 to 100 °C, and the theoretical weight loss is 14.40 wt.%. The theoretical bound water content of $CuSO_4 \cdot 5H_2O$ under the TGA method is 14.40 + 14.40 = 28.80 wt.%. The bound water content measured via the TGA method is 28.35 wt.%. Therefore, the relative error in measuring $CuSO_4 \cdot 5H_2O$ using the TGA method is (28.80−28.35)/28.80 = 1.56%.

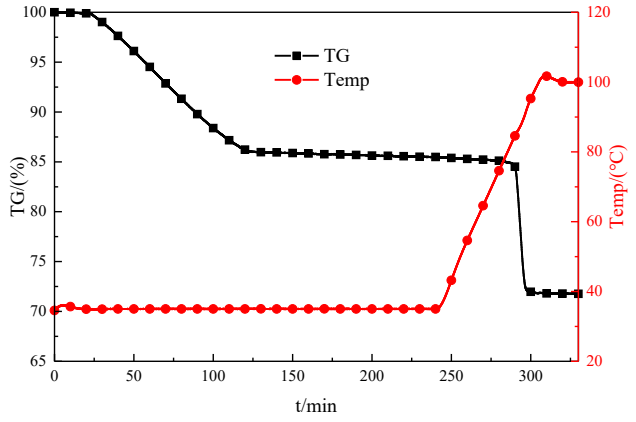

(**a**)

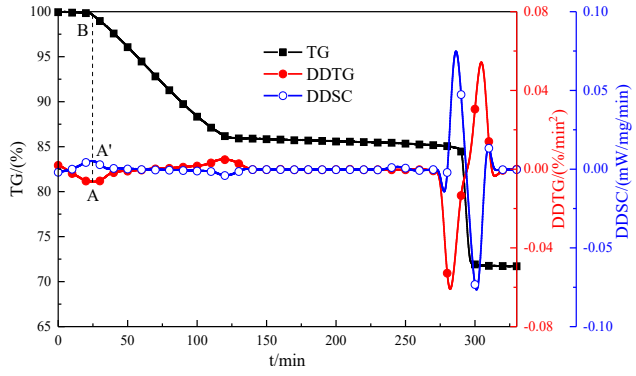

(**b**)

Figure A2. Thermal analysis results of $CuSO_4 \cdot 5H_2O$ sample. (**a**) Raw data for thermal analysis of $CuSO_4 \cdot 5H_2O$ sample; (**b**) thermal analysis data processing of $CuSO_4 \cdot 5H_2O$ sample.

Appendix B

The electrical power P_0 consumed by the device is measured and recorded using a power meter. The detailed measurement results are shown in Table A1.

Table A1. Measurement results of the electric power.

P (W)	P_0 (W)
500	329
600	364
700	399
800	437

Note: P is the setting microwave power (W).

The real output power P_{real} of the microwave device is measured according to GB/T 18800-2017, and the detailed measurement steps are as follows:

At the beginning of the experiment, the cylindrical borosilicate glass container is at room temperature, and the initial temperature of water is within the range of 10 ± 1 °C. The temperature of the water is quickly measured before the water is poured into the container. Add 1000 ± 5 g of water into the container and place the container in the corresponding position. Run the microwave oven and measure the time required for the water temperature to reach 20 ± 2 °C. Once the desired temperature is achieved, then cut off the power and measure the final temperature of the water within 60 s. Stir the water before measuring the final temperature of the water during the experiment. The stirring rod is made of material with low heat capacity.

The real output power P_{real} can be calculated as follows:

$$P_{real} = [4.19m_w(T_f - T_i) + 0.55m_c(T_f - T_i)]/t \quad \text{(A4)}$$

where P_{real} is the real output power (W), m_w is the mass of the water (g), m_c is the mass of the glass container (g), T_i is the initial temperature of the water (°C), T_f is the final temperature of the water (°C), t is the heating time (s), and the specific heat capacities of water and glass container are 4.19 J/(g·°C) and 0.55 J/(g·°C), respectively.

Table A2 presents the measurement results of the real output power.

Table A2. Measurement results of the real output power.

P (W)	m_c (g)	m_w (g)	T_i (°C)	T_f (°C)	t (s)	P_{real} (W)
500	270	1000	10	20	314	138
600	270	999	10	20	217	200
700	270	1000	10	20	175	248
800	270	1001	10	21	133	359

Note: P is the setting microwave power (W).

References

1. Chen, Z.; Afzal, M.T.; Salema, A.A. Microwave Drying of Wastewater Sewage Sludge. *J. Clean Energy Technol.* **2014**, *2*, 282–286. [CrossRef]
2. Guo, H.; Tan, Z.; Li, H.; Long, Y.; Ji, A.; Liu, L. Dynamic Characteristics Analysis of Metallurgical Waste Heat Radiative Drying of Thin Layers of Sewage Sludge. *Processes* **2023**, *11*, 2535. [CrossRef]
3. Djandja, O.S.; Wang, Z.; Wang, F.; Xu, Y.P.; Duan, P.G. Pyrolysis of Municipal Sewage Sludge for Biofuel Production: A Review. *Ind. Eng. Chem. Res.* **2020**, *59*, 16939–16956. [CrossRef]
4. Migliaccio, R.; Brachi, P.; Montagnaro, F.; Papa, S.; Urciuolo, M. Sewage Sludge Gasification in a Fluidized Bed: Experimental Investigation and Modeling. *Ind. Eng. Chem. Res.* **2021**, *60*, 5034–5047. [CrossRef]
5. Zhang, X.; Li, X.; Li, R.; Wu, Y. Hydrothermal Carbonization and Liquefaction of Sludge for Harmless and Resource Purposes: A Review. *Energy Fuel* **2020**, *34*, 13268–13290. [CrossRef]
6. Norinaga, K.; Kumagai, H.; Hayashi, J.; Chiba, T. Classification of Water Sorbed in Coal on the Basis of Congelation Characteristics. *Energy Fuel* **1998**, *12*, 574–579. [CrossRef]

7. Allardice, D.J.; Evans, D.G. The-brown coal/water system. Part 2. Water sorption isotherms on bed-moist Yallourn brown coal. *Fuel* **1971**, *50*, 236–253. [CrossRef]
8. Karthikeyan, M.; Wu, Z.; Mujumdar, A.S. Low-Rank Coal Drying Technologies—Current Status and New Developments. *Dry. Technol.* **2009**, *27*, 403–415. [CrossRef]
9. Chen, D.; Jiang, Y.; Jiang, X.; Ma, Z.; Yan, J.; Cen, K.; Yu, X.; Liao, H.; Zhao, H. The effect of anionic dispersants on the moisture distribution of a coal water slurry. *Fuel Process Technol.* **2014**, *126*, 122–130. [CrossRef]
10. Vaxelaire, J.; Cézac, P. Moisture distribution in activated sludges: A review. *Water Res.* **2004**, *38*, 2215–2230. [CrossRef]
11. Robinson, J.; Knocke, W.R. Use of dilatometric and drying techniques for assessing sludge dewatering characteristics. *Water Environ. Res.* **1992**, *64*, 60–68. [CrossRef]
12. Tsang, K.R.; Vesilind, P.A. Moisture distribution in sludges. *Waterence Technol.* **1990**, *22*, 135–142. [CrossRef]
13. Smollen, M. Evaluation of municipal sludge drying and dewatering with respect to sludge volume reduction. *Waterence Technol.* **1990**, *22*, 153–161. [CrossRef]
14. Deng, W.; Li, X.; Yan, J.; Wang, F.; Chi, Y.; Cen, K. Moisture distribution in sludges based on different testing methods. *J. Environ. Sci.* **2011**, *23*, 6. [CrossRef]
15. Fraikin, L.; Salmon, T.; Herbreteau, B.; Levasseur, J.P.; Nicol, F.; Crine, M.; Léonard, A. Impact of Storage Duration on the Gaseous Emissions during Convective Drying of Urban Residual Sludges. *Chem. Eng. Technol.* **2011**, *34*, 1172–1176. [CrossRef]
16. Deng, W.Y.; Yan, J.H.; Li, X.D.; Wang, F.; Lu, S.Y.; Chi, Y.; Cen, K.F. Measurement and simulation of the contact drying of sewage sludge in a Nara-type paddle dryer. *Chem. Eng. Sci.* **2009**, *64*, 5117–5124. [CrossRef]
17. Ferrasse, J.H.; Arlabosse, P.; Lecomte, D. Heat, momentum, and mass transfer measurements in indirect agitated sludge dryer. *Dry. Technol.* **2002**, *20*, 749–769. [CrossRef]
18. Yan, J.H.; Deng, W.Y.; Li, X.D.; Wang, F.; Chi, Y.; Lu, S.Y.; Cen, K.F. Experimental and Theoretical Study of Agitated Contact Drying of Sewage Sludge under Partial Vacuum Conditions. *Dry. Technol.* **2009**, *27*, 787–796. [CrossRef]
19. Cieslik, B.M.; Namiesnik, J.; Konieczka, P. Review of sewage sludge management: Standards, regulations and analytical methods. *J. Clean. Prod.* **2015**, *90*, 1–15. [CrossRef]
20. Pickles, C.A.; Gao, F.; Kelebek, S. Microwave drying of a low-rank sub-bituminous coal. *Miner. Eng.* **2014**, *62*, 31–42. [CrossRef]
21. Xinzhi, Z.; Lun, S.; Ke, C.; Yang, Y.; Yu, Z.; Ruobin, Z. Research on multi-stage power control system of lignite microwave drying production line. *CIESC J.* **2018**, *69*, 274–282.
22. Bennamoun, L.; Chen, Z.; Afzal, M.T. Microwave drying of wastewater sludge: Experimental and modeling study. *Dry. Technol.* **2016**, *34*, 235–243. [CrossRef]
23. Song, Z.; Jing, C.; Yao, L.; Zhao, X.; Wang, W.; Mao, Y.; Ma, C. Microwave drying performance of single-particle coal slime and energy consumption analyses. *Fuel Process Technol.* **2016**, *143*, 69–78. [CrossRef]
24. Song, Z.; Yao, L.; Jing, C.; Zhao, X.; Wang, W.; Sun, J.; Mao, Y.; Ma, C. Elucidation of the Pumping Effect during Microwave Drying of Lignite. *Ind. Eng. Chem. Res.* **2016**, *55*, 3167–3176. [CrossRef]
25. Fu, B.A.; Chen, M.Q.; Song, J.J. Investigation on the microwave drying kinetics and pumping phenomenon of lignite spheres. *Appl. Therm. Eng.* **2017**, *124*, 371–380. [CrossRef]
26. Elenga, R.G.; Massamba, D.; Niéré, R.R.; Maniongui, J.G.; Dirras, G. Convective and Microwave Dryings of Raffia Fruit: Modeling and Effects on Color and Hardness. *Res. J. Appl. Sci. Eng. Technol.* **2013**, *6*, 2715–2723. [CrossRef]
27. Bantle, M.; K Fer, T.; Eikevik, T.M. Model and process simulation of microwave assisted convective drying of clipfish. *Appl. Therm. Eng.* **2013**, *59*, 675–682. [CrossRef]
28. Domínguez, A.; Menéndez, J.A.; Inguanzo, M.; Pis, J.J. Sewage sludge drying using microwave energy and characterization by IRTF. *Afinidad* **2004**, *61*, 280–285.
29. Fang, L.; Li, S.; Zhai, T.; Zhao, X.; Sun, H. A comparative study on the drying process of sewage sludge: Microwave and air-blast. In Proceedings of the International Conference on Civil, Transportation and Environmental Engineering (CTEE 12), Kuala Lumpur, Malaysia, 1–2 December 2013.
30. Song, Z.L.; Yao, L.S.; Jing, C.M.; Zhao, X.Q.; Wang, W.L.; Ma, C.Y. Drying behavior of lignite under microwave heating. *Dry. Technol.* **2017**, *35*, 433–443. [CrossRef]
31. Shen, L.Y.; Zhu, Y.; Liu, C.H.; Wang, L.; Liu, H.; Kamruzzaman, M.; Liu, C.; Zhang, Y.P.; Zheng, X.Z. Modelling of moving drying process and analysis of drying characteristics for germinated brown rice under continuous microwave drying. *Biosyst. Eng.* **2020**, *195*, 64–88. [CrossRef]
32. Wei, Q.Y.; Huang, J.P.; Zhang, Z.Y.; Lia, D.J.; Liu, C.Q.; Xiao, Y.D.; Lagnika, C.; Zhang, M. Effects of different combined drying methods on drying uniformity and quality of dried taro slices. *Dry. Technol.* **2019**, *37*, 322–330. [CrossRef]
33. Wang, Y.; Zhang, M.; Mujumdar, A.S.; Mothibe, K.J.; Roknul Azam, S.M. Study of drying uniformity in pulsed spouted microwave–vacuum drying of stem lettuce slices with regard to product quality. *Dry. Technol.* **2013**, *31*, 91–101. [CrossRef]
34. Hii, C.L.; Ong, S.P.; Yap, J.Y.; Putranto, A.; Mangindaan, D. Hybrid drying of food and bioproducts: A review. *Dry. Technol.* **2021**, *39*, 1554–1576. [CrossRef]
35. Tahmasebi, A.; Yu, J.; Han, Y.; Zhao, H.; Bhattacharya, S. A kinetic study of microwave and fluidized-bed drying of a Chinese lignite. *Chem. Eng. Res. Des.* **2014**, *92*, 54–65. [CrossRef]
36. Li, L.; Jiang, X.; Qin, X.; Yan, K.; Chen, J.; Feng, T.; Wang, F.; Song, Z.; Zhao, X. Experimental study and energy analysis on microwave-assisted lignite drying. *Dry. Technol.* **2019**, *37*, 962–975. [CrossRef]

37. Ge, J.; He, Y.; Zhu, Y.; Wang, Z.; Zhang, K.; Huang, Z.; Cen, K. Combined conventional thermal and microwave drying process for typical Chinese lignite. *Dry. Technol.* **2019**, *37*, 813–823. [CrossRef]
38. Li, L.; Xiaowei, J.; Zhiguo, B.; Jianwei, W.; Fumao, W.; Zhanlong, S.; Xiqiang, Z.; Chunyuan, M. Microwave drying performance of lignite with the assistance of biomass-derived char. *Dry. Technol.* **2019**, *37*, 173–185. [CrossRef]
39. Idris, A.; Khalid, K.; Omar, W. Drying of silica sludge using microwave heating. *Appl. Therm. Eng.* **2004**, *24*, 905–918. [CrossRef]
40. Mawioo, P.M.; Rweyemamu, A.; Garcia, H.A.; Hooijmans, C.M.; Brdjanovic, D. Evaluation of a microwave based reactor for the treatment of blackwater sludge. *Sci. Total Environ.* **2016**, *548*, 72–81. [CrossRef]
41. Zhao, P.; Liu, C.; Qu, W.; He, Z.; Gao, J.; Jia, L.; Ji, S.; Ruan, R. Effect of Temperature and Microwave Power Levels on Microwave Drying Kinetics of Zhaotong Lignite. *Processes* **2019**, *7*, 74. [CrossRef]
42. Fu, B.A.; Chen, M.Q.; Huang, Y.W.; Luo, H.F. Combined effects of additives and power levels on microwave drying performance of lignite thin layer. *Dry. Technol.* **2017**, *35*, 227–239. [CrossRef]
43. Lin, B.; Cao, X.; Liu, T.; Ni, Z.; Wang, Z. Experimental Research on Water Migration-Damage Characteristics of Lignite under Microwave Heating. *Energy Fuel* **2021**, *35*, 1058–1069.
44. Wang, Z.; Sun, J.; Chen, F.; Liao, X.; Hu, X. Mathematical modelling on thin layer microwave drying of apple pomace with and without hot air pre-drying. *J. Food Eng.* **2007**, *80*, 536–544. [CrossRef]
45. Ni, H.; Datta, A.K.; Torrance, K.E. Moisture transport in intensive microwave heating of biomaterials: A multiphase porous media model. *Int. J. Heat. Mass. Transf.* **1999**, *42*, 1501–1512. [CrossRef]
46. Dincov, D.D.; Parrott, K.A.; Pericleous, K.A. Heat and mass transfer in two-phase porous materials under intensive microwave heating. *J. Food Eng.* **2004**, *65*, 403–412. [CrossRef]
47. Wang, B.H. Review of drying kinetics. *Dry. Technol. Equip.* **2009**, *7*, 6.
48. Han, R.; Zhou, A.; Zhang, N.; Li, Z. A review of kinetic studies on evaporative dehydration of lignite. *Fuel* **2022**, *329*, 125445–125457. [CrossRef]
49. Zhu, J.; Liu, J.; Wu, J.; Cheng, J.; Zhou, J.; Cen, K. Thin-layer drying characteristics and modeling of Ximeng lignite under microwave irradiation. *Fuel Process Technol.* **2015**, *130*, 62–70. [CrossRef]
50. Araszkiewicz, M.; Koziol, A.; Lupinska, A.; Lupinski, M. Temperature distribution in a single sphere dried with microwaves and hot Air. *Dry. Technol.* **2006**, *24*, 1381–1386. [CrossRef]
51. Cui, Z.; Xu, S.; Sun, D.; Chen, W. Temperature changes during microwave-vacuum drying of sliced carrots. *Dry. Technol.* **2005**, *23*, 1057–1074. [CrossRef]
52. Putranto, A.; Chen, X.D. Reaction engineering approach modeling of intensified drying of fruits and vegetables using microwave, ultrasonic and infrared-heating. *Dry. Technol.* **2020**, *38*, 747–757. [CrossRef]
53. Putranto, A.; Chen, X.D. Multiphase modeling of intermittent drying using the spatial reaction engineering approach (S-REA). *Chem. Eng. Process. Process Intensif.* **2013**, *70*, 169–183.
54. Putranto, A.; Chen, X.D. A simple and effective model for modeling of convective drying of sewage sludge: The reaction engineering approach (REA). *Procedia Chem.* **2014**, *9*, 77–87. [CrossRef]
55. Putranto, A.; Chen, X.D. Microwave drying at various conditions modeled using the reaction engineering approach (REA). *Dry. Technol.* **2016**, *34*, 1654–1663. [CrossRef]
56. Hatibaruah, D.; Baruah, D.C.; Sanyal, A.S. Microwave drying characteristics of assam CTC tea (*Camellia assamica*). *J. Food Process Pres.* **2013**, *37*, 366–370. [CrossRef]
57. Kantrong, H.; Tansakul, A.; Mittal, G.S. Drying characteristics and quality of shiitake mushroom undergoing microwave-vacuum drying and microwave-vacuum combined with infrared drying. *J. Food Sci. Technol.* **2014**, *51*, 3594–3608.
58. Arslan, D.; Zcan, M.M. Study the effect of sun, oven and microwave drying on quality of onion slices. *LWT Food Sci. Technol.* **2010**, *43*, 1121–1127. [CrossRef]
59. Hacifazlioglu, H. Comparison of Efficiencies of Microwave and Conventional Electric Ovens in the Drying of Slime-Coal Agglomerates. *Int. J. Coal Prep. Util.* **2017**, *37*, 169–178. [CrossRef]
60. Guo, J.; Zheng, L.; Li, Z. Microwave drying behavior, energy consumption, and mathematical modeling of sewage sludge in a novel pilot-scale microwave drying system. *Sci. Total Environ.* **2021**, *777*, 146109–146118. [CrossRef] [PubMed]
61. Cheng, L.; Li, W.; Li, Y.; Yang, Y.; Li, Y.; Cheng, Y.; Song, D. Thermal analysis and decomposition kinetics of the dehydration of copper sulfate pentahydrate. *J. Therm. Anal. Calorim.* **2019**, *135*, 2697–2703. [CrossRef]
62. Li, C.; Liao, J.; Yin, Y.; Mo, Q.; Chang, L.; Bao, W. Kinetic analysis on the microwave drying of different forms of water in lignite. *Fuel Process Technol.* **2018**, *176*, 174–181. [CrossRef]
63. Zarein, M.; Samadi, S.H.; Ghobadian, B. Investigation of microwave dryer effect on energy efficiency during drying of apple slices. *J. Saudi Soc. Agric. Sci.* **2015**, *14*, 41–47. [CrossRef]
64. Guo, Z.; Li, F.; Su, G.; Zhai, D.; Liu, C. Microwave drying of nickel-containing residue: Dielectric properties, kinetics, and energy aspects. *Green. Process Synth.* **2019**, *8*, 814–824. [CrossRef]
65. Zhu, B.C.; Song, W.D.; Fang, D.Y.; Lu, D.Q. Multicomponent diffusion model of porous catalyst efficiency factor (I) Multicomponent diffusion model and numerical calculation method. *CIESC J.* **1984**, *1*, 33–40.

66. Özbek, B.; Dadali, G. Thin-layer drying characteristics and modelling of mint leaves undergoing microwave treatment. *J. Food Eng.* **2007**, *83*, 541–549. [CrossRef]
67. Song, Z.; Jing, C.; Yao, L.; Zhao, X.; Sun, J.; Wang, W.; Mao, Y.; Ma, C. Coal slime hot air/microwave combined drying characteristics and energy analysis. *Fuel Process Technol.* **2017**, *156*, 491–499. [CrossRef]